The Astronomical Journal, 148:110 (6pp), 2014 December doi:10.1088/0004-6256/148/6/110

SIX-YEAR OPTICAL MONITORING OF THE BL LACERTAE OBJECT 1ES 0806+52.4

Zhongyi Man[1], Xiaoyuan Zhang[1], Jianghua Wu[1], Xu Zhou[2], and Qirong Yuan[3]
[1] Department of Astronomy, Beijing Normal University, Beijing 100875, China; jhwu@bnu.edu.cn
[2] Key Laboratory of Optical Astronomy, National Astronomical Observatories, Chinese Academy of Sciences, 20A Datun Road, Beijing 100012, China
[3] Department of Physics and Institute of Theoretical Physics, Nanjing Normal University, Nanjing 210046, China
Received 2014 March 25; accepted 2014 August 2; published 2014 October 30

ABSTRACT

We present the results of the first systematic long-term multicolor optical monitoring of the BL Lacertae object 1ES 0806+52.4. The monitoring was performed in multiple passbands with a 60/90 cm Schmidt telescope from 2005 December to 2011 February. The overall brightness of this object decreased from 2005 December to 2008 December but was regained after that. A sharp outburst probably occurred around the end of our monitoring program. Overlapping the long-term trend are some short-term small-amplitude oscillations. No intranight variability was found in the object, which is in accordance with the historical observations before 2005. By investigating the color behavior, we found a strong bluer-when-brighter chromatism for the long-term variability of 1ES 0806+52.4. The total amplitudes at the *c, i,* and *o* bands are 1.18, 1.12, and 1.02 mag, respectively. The amplitudes tend to increase toward shorter wavelengths, which may be a major cause of the bluer-when-brighter chromatism. Such bluer-when-brighter chromatisms are also found in other blazars, such as S5 0716+714, OJ 287. The hard-X-ray data collected from the *Swift*/BAT archive was correlated with our optical data. No positive result was found, the reason for which may be that the hard-X-ray flux is a combination of the synchrotron and inverse Compton emission, but with different timescales and cadences under the leptonic synchrotron self-Compton model.

Key words: BL Lacertae objects: individual (1ES 0806+524) – galaxies: active – galaxies: photometry

Online-only material: machine-readable and VO tables

1. INTRODUCTION

Active galactic nuclei (AGNs) are powered by supermassive black holes surrounded by accretion disks. Blazar, one of the most violently variable classes of AGNs, are distinguished by large and rapid flux variability (Bonning et al. 2012; Sandrinelli et al. 2014), high and variable polarization (Hagen-Thorn et al. 2008; Sasada et al. 2008; Gaur et al. 2014), and, basically, a nonthermal continuum. Depending on the presence of strong emission lines in spectrum, a blazar can be further termed either a flat-spectrum radio quasar (FSRQ) or a BL Lacerate object.

Two typical components can be seen in the spectral energy distribution (SED) of blazars: one at low frequencies from radio to UV or soft X-rays and the other that ranges from X-rays to gamma-rays (e.g., Takahashi 2001; Bonning et al. 2012). The low energy component is believed to be caused by the synchrotron process of the relativistic particles in the jet. The high energy one, however, is interpreted as either being due to inverse Compton scattering of the low-energy photons by the same ensemble of relativistic electrons responsible for the synchrotron emission named the synchrotron self-Compton model (e.g., Mücke et al. 2003; Krawczynski et al. 2002), or due to the hadronic processes initiated by the synchrotron radiation of protons co-accelerated with the electrons in the jet (hadronic models, e.g., Mücke & Protheroe 2001; Levinson 2006).

1ES 0806+52.4 was identified as a BL Lac object (Schachter et al. 1993) based on the observations carried out on both radio bands from the Green Bank 91 m telescope (Becker et al. 1991) and X-ray bands from the Einstein Slew Survey (Elvis et al. 1992). The redshift of its host galaxy is estimated as $z = 0.138$ (Bade et al. 1998). Very-high-energy gamma-ray observations of 1ES 0806+52.4 were reported by the Whipple Collaboration (de la Calle Pérez et al. 2003; Horan et al. 2004), the HEGRA Collaboration (Aharonian et al. 2004) and VERITAS (Weekes et al. 2002). *R*-band optical observations of this BL Lac object were conducted from 2000 to 2001 (Kurtanidze et al. 2002), and from 2002 to 2004 (Kapanadze 2009). The former highlighted the variability with one magnitude on long timescales (Kurtanidze et al. 2002). Until now, no long-term systematic optical monitoring has been conducted on this object, and no research has been made on the correlation between radiation at different wavelengths.

Our quasi-simultaneous multicolor monitoring of 1ES 0806+52.4 was carried out from 2005 December to 2011 February. In order to investigate the correlation between the optical and the hard-X-ray emission, X-ray data covering the same period were collected from the *Swift*/Burst Alert Telescope (BAT) data archive and were analyzed with the optical data.

2. OBSERVATION AND DATA REDUCTION

Our observations were performed using the 60/90 cm Schmidt telescope at the Xinglong Station of the National Astronomical Observatories of China (NAOC). Mounted at the telescope main focus was a Ford Aerospace 2048 × 2048 thick CCD camera, which was then surrogated by a new E2V 4096 × 4096 CCD in 2006 December. The field of view is enlarged from $58' \times 58'$ to $96' \times 96'$. The resolution is increased from $1''.7$ pixel^{-1} to $1''.3$ pixel^{-1}. The blue quantum efficiency of the new E2V thinned CCD is also higher than the former thick one. The telescope is equipped with 15 color intermediate-band filters, covering a wavelength range from 3000 to 10,000 Å (Fan et al. 1996). Four F sub-dwarfs (Oke & Gunn 1983) are used as standard stars to calibrate the magnitude. For the details of the filter system, such as the definition of the corresponding magnitudes and how to derive flux from the magnitude, one can refer to Yan et al. (2000), Zhou et al. (2001, 2003).

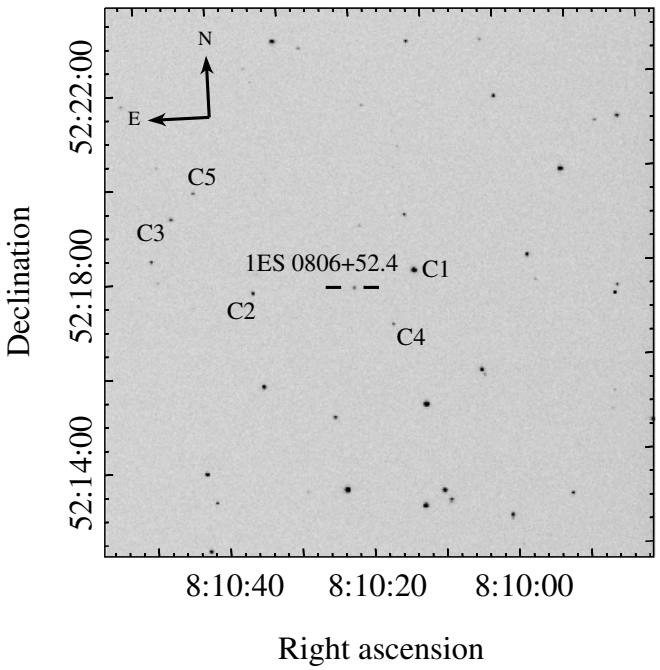

Figure 1. Finding chart of 1ES 0806+52.4 and the five comparison stars taken in *i* band with the 60/90 Schmidt telescope on 2007 February 5. The size is $12' \times 12'$ (or 512×512 in pixels).

Our monitoring program on 1ES 0806+52.4 started on the night of 2005 December 12 and ended on 2011 February 11. After ruling out the nights with bad weather conditions and those for other targets, the actual number of observation nights is 77. Filters in the *e, i,* and *m* bands were adopted between 2005 and 2006. During most of the nights in this period, more than 10 exposures, sometimes up to 20, were made in each band with a temporal resolution of about 20 minutes. Filters were then surrogated by *c, i,* and *o* bands from the end of 2006 December to 2011 February, and less than 10 exposures were made on most nights. The exposure time determined by the moon phase, weather conditions, and the filter varies from 60 to 540 s. The central wavelengths of the *c, e, i, m,* and *o* bands are 4210, 4920, 6660, 8020, and 9190 Å, respectively. The *i* magnitude can be transformed into the broadband *R* magnitude for stars by using the formula given by Zhou et al. (2003) and for AGNs by using the formula given by Dai et al. (2013).

We performed bias subtraction and flat-fielding using the BATC automatic data reduction software PIPELINE I (Fan et al. 1996; Zheng et al. 1999). Four stars, C1, C2, C3, and C4 (see Figure 1), were selected as reference stars (Fiorucci et al. 1998), and we chose star C5 as a check star (for a reasonable selection of reference and check stars, see Howell et al. 1988). We extracted the instrumental aperture magnitudes of the blazar and the five comparison stars from each frame by using the algorithm of Stetson (1987). The radii of the aperture and the sky annuli were adopted as 3, 7, and 10 pixels, respectively, and they may be adjusted slightly according to the seeing. The brightness of the blazar was measured relative to the average magnitude of the four reference stars. The accuracy of our measurement is shown by the check star's differential magnitude, the difference between the magnitude of C5 and the average magnitude of the four reference stars. We observed stars C1, C2, C3, C4, and C5 on a photometric night, and used the photometric F-type standard stars mentioned above to calibrate their standard magnitudes. The results are listed in Table 1.

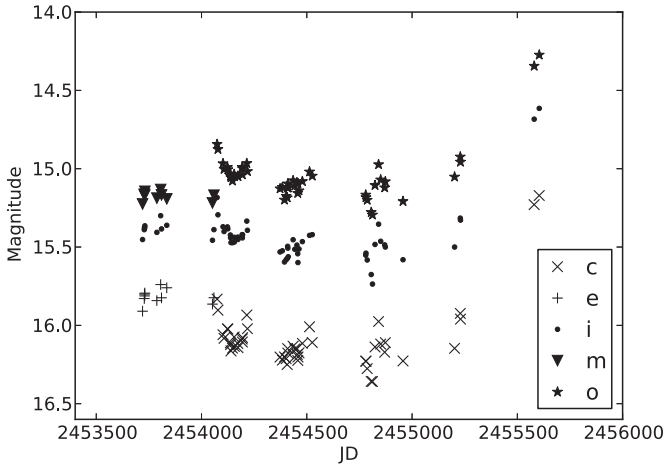

Figure 2. Nightly average light curves of 1ES 0806+52.4 in the *c*, *e*, *i*, *m*, and *o* bands.

Table 1
Magnitude of Five Comparison Stars

Band	C1	C2	C3	C4	C5
c	14.035	15.410	15.379	16.498	16.187
e	13.291	14.859	14.938	15.901	15.809
i	12.653	14.349	14.534	15.412	15.548
m	12.476	14.216	14.420	15.245	15.256
o	12.387	14.164	14.402	15.170	15.399

3. LIGHT CURVE

The samples of observational log and results are given in Tables 2–6. The columns include observation date and time in universal time, exposure time in seconds, Julian date, magnitude, error, and differential magnitude of star C5 (its nightly averages were set to zero).

We gathered 1399 optical data points in total: numbers of photometric points for *c, e, i, m,* and *o* bands are 292, 150, 490, 171 and 296, respectively. The light curves of the overall monitoring period in five bands are shown in Figure 2. There are basically two outbursts with a concave shape between them. The peak of the first outburst occurred on 2006 March 15 (JD 2,453,810), and then the brightness of the object started declining until 2008 December 11 (JD 2,454,812). Later on, the curves turned up to the second outburst, which is more powerful than the first one. No details can be known about the strong outburst because our observation ceased on 2011 February 11 (JD 2,455,604). Overlapped on the long-term large-amplitude variations are some short-term small-amplitude oscillations during JD 2,454,000 to JD 2,455,000. We also notice that a double-peak structure of 1ES 0806+52.4 was spotted between 2002 and 2004 (Kapanadze 2009), yet it was not found in our observations.

The overall amplitudes in *e, i,* and *m* bands from 2005 December 15 to 2006 November 19 are 0.17, 0.12, and 0.09 mag, respectively, the amplitudes in *c, i,* and *o* bands from 2006 December 4 to 2011 February 11 are 1.18, 1.12, and 1.02 mag. We note that the overall amplitudes tend to decline with the decreasing frequency. We examined the intranight variability of this object by using the methods suggested by de Diego (2010), but found no obvious intranight variability during the whole timespan. It is in accordance with the observation from 2002 to 2004 (Kapanadze 2009), which detected no intranight variability for this source either. Nevertheless, our average

Table 2
Observational Log and Results in the *c* Band

Observation Date (UT)	Observation Time (UT)	Exposure Time (s)	Julian Date JD	c (mag)	c_{err} (mag)	dfmagC5 (mag)
2006 Dec 4	18:44:51.0	480	2454074.28115	15.886	0.034	0.064
2006 Dec 4	19:07:27.0	480	2454074.29684	15.806	0.035	−0.011
2006 Dec 4	19:29:52.0	480	2454074.31241	15.809	0.031	0.008
2006 Dec 4	19:52:18.0	480	2454074.32799	15.832	0.032	0.012
2006 Dec 4	20:14:53.0	480	2454074.34367	15.850	0.037	−0.006

(This table is available in its entirety in machine-readable and Virtual Observatory (VO) forms in the online journal. A portion is shown here for guidance regarding its form and content.)

Table 3
Observational Log and Results in the *e* Band

Observation Date (UT)	Observation Time (UT)	Exposure Time (s)	Julian Date JD	e (mag)	e_{err} (mag)	dfmagC5 (mag)
2005 Dec 15	15:01:46.0	300	2453720.12623	15.991	0.085	−0.024
2005 Dec 15	15:17:43.0	300	2453720.13730	15.993	0.078	0.106
2005 Dec 15	15:34:01.0	300	2453720.14862	15.925	0.081	−0.056
2005 Dec 15	15:49:56.0	300	2453720.15968	15.894	0.083	−0.053
2005 Dec 15	16:05:54.0	300	2453720.17076	15.865	0.071	−0.071

(This table is available in its entirety in machine-readable and Virtual Observatory (VO) forms in the online journal. A portion is shown here for guidance regarding its form and content.)

Table 4
Observational Log and Results in the *i* Band

Observation Date (UT)	Observation Time (UT)	Exposure Time (s)	Julian Date JD	i (mag)	i_{err} (mag)	dfmagC5 (mag)
2005 Dec 12	15:44:16.0	180	2453717.15574	15.488	0.034	−0.021
2005 Dec 12	15:55:15.0	180	2453717.16337	15.514	0.033	0.006
2005 Dec 12	16:05:08.0	180	2453717.17023	15.408	0.030	−0.004
2005 Dec 12	16:15:18.0	180	2453717.17729	15.416	0.030	−0.024
2005 Dec 12	16:25:24.0	180	2453717.18431	15.408	0.028	0.042

(This table is available in its entirety in machine-readable and Virtual Observatory (VO) forms in the online journal. A portion is shown here for guidance regarding its form and content.)

Table 5
Observational Log and Results in the *m* Band

Observation Date (UT)	Observation Time (UT)	Exposure Time (s)	Julian Date JD	m (mag)	m_{err} (mag)	dfmagC5 (mag)
2005 Dec 12	15:49:15.0	300	2453717.15920	15.248	0.044	0.014
2005 Dec 12	16:00:10.0	300	2453717.16678	15.238	0.041	−0.057
2005 Dec 12	16:10:21.0	300	2453717.17385	15.189	0.040	0.053
2005 Dec 12	16:20:26.0	300	2453717.18086	15.236	0.045	−0.019
2005 Dec 12	16:30:24.0	300	2453717.18778	15.264	0.051	−0.006

(This table is available in its entirety in machine-readable and Virtual Observatory (VO) forms in the online journal. A portion is shown here for guidance regarding its form and content.)

Table 6
Observational Log and Results in the *o* Band

Observation Date (UT)	Observation Time (UT)	Exposure Time (s)	Julian Date JD	o (mag)	o_{err} (mag)	dfmagC5 (mag)
2006 Dec 04	18:57:10.0	480	2454074.28970	14.818	0.027	−0.063
2006 Dec 4	19:20:16.0	540	2454074.30574	14.840	0.028	−0.040
2006 Dec 4	19:42:41.0	540	2454074.32131	14.822	0.026	−0.026
2006 Dec 4	20:05:09.0	540	2454074.33691	14.809	0.026	−0.009
2006 Dec 4	20:27:41.0	540	2454074.35256	14.840	0.027	0.006

(This table is available in its entirety in machine-readable and Virtual Observatory (VO) forms in the online journal. A portion is shown here for guidance regarding its form and content.)

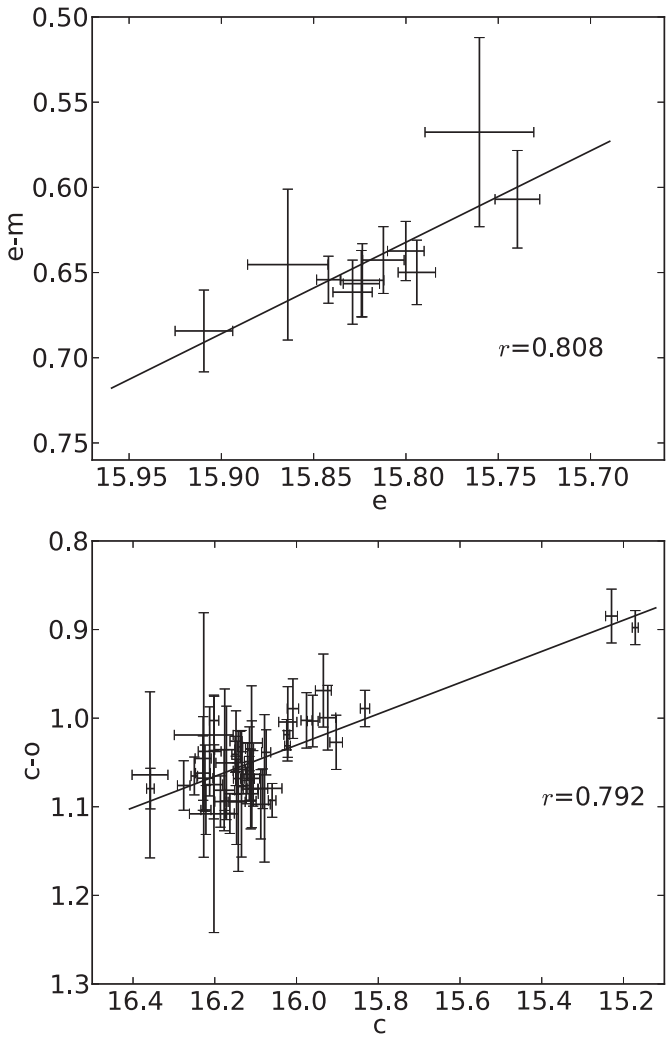

Figure 3. Long-term color behavior of the first (up) and the second (bottom) stages. The nightly average data are used. Strong bluer-when-brighter chromatisms can be found.

observational duration on each night is only 3.6 hr, which may not be long enough to detect the intranight variability, if there are some cases. Some blazars display strong intranight variability. For example, S5 0716+714 was observed to vary by 0.117 mag in 1.1 hr (Dai et al. 2013). PKS 2155-304 was detected to have a very fast variability rate of 0.43 mag/h in the observation session (Sandrinelli et al. 2014).

4. COLOR BEHAVIOR

The long-term color behavior of 1ES 0806+52.4 was investigated based on our data. We adopted the *e* and *m* bands to calculate the color in the first stage from 2005 to 2006, and used the *c* and *o* bands in the second stage from 2006 to 2011. This is because the differences in wavelength of the two pairs of filters are relatively large, and can thereby denote a better spectral shape. The color–magnitude diagrams are displayed in Figure 3.

The linear least square method with measurement errors taken into consideration was used to fit the points. The points in the left panel for the first stage have a linear regression of $y = 0.537x–7.847$, and the correlation coefficient is 0.808, which means a significance level of 95%. The points in the right panel for the second stage have a linear regression of $y = 0.176x–1.791$, and the correlation coefficient is 0.792, which also means a significance level of 95%. Both panels show strong bluer-when-brighter (BWB) chromatisms. The intranight color behavior of 1ES 0806+52.4 was not investigated due to the absence of intranight variability.

A number of BL Lac objects have been reported displaying the BWB phenomenon thus far. Significant BWB correlations were found for both internight and intranight variations in the typical BL Lac object S5 0714+716 (e.g., Wu et al. 2005). Internight BWB was found in BL Lacerate (e.g., Zhai & Wei 2012). In OJ 287, a well-studied BL Lac, BWB is also found on a long time scale (Dai et al. 2011). In fact, such a BWB chromatism is likely to be a general feature of BL Lac objects (e.g., Vagnetti et al. 2003; Rani et al. 2010). For FSRQ, there were once claims of a redder-when-brighter trend (e.g., Gu et al. 2006; Hu et al. 2006). However, Gu & Ai (2011) found evidence of this color behavior for only one object in a sample of 29 FSRQs. The mechanism of BWB was simulated (Dai et al. 2011), and the result shows that BWB is probably due to the difference of the amplitude at different wavelengths. The variation amplitude of 1ES 0806+52.4 was found to decrease with decreasing frequency, which can at least partly explain the BWB behavior observed in this object.

5. CROSS-CORRELATION ANALYSIS AND DISCUSSIONS

In order to research the emission at different wavelengths, our optical data was compared with the timeseries data provided by the *Swift*/BAT, which has monitored 1ES 0806+52.4 in the hard-X-ray band since 2005. The *Swift*/BAT hard-X-ray transient monitor provides near-real-time coverage of the X-ray sky in the energy range of 15–50 keV, or 3.63×10^{18}–1.21×10^{19} Hz in frequency. The BAT observes 88% of the sky each day with a detection sensitivity of 5.3 mCrab for a full-day observation and a time resolution as fine as 64 s (Krimm et al. 2013). We used the daily average data offered by *Swift*/BAT. Both sequences were transformed into flux so that we could analyze them together. The light curves of the *i* band and X-ray band are shown in Figure 4.

We used the *z*-transformed discrete correlation functions (ZDCFs; Alexander 1997) to search for the optical hard-X-ray correlations. The ZDCF differs from the discrete correlation function (DCF; Edelson & Krolik 1988) because it bins the data points into equal population bins and uses Fishers *z* transform to stabilize the highly skewed distribution of the correlation coefficient. It is much more efficient than the DCF at uncovering correlations involving the variability timescale, and deals with under-sampled light curves better than both the DCF and the interpolated cross-correlation function (Gaskell & Peterson 1987). The results are displayed in Figure 5 for all of the data from JD 2,453,717 to JD 2,455,604.

In Figure 5, no obvious peak of the DCF values can be found, indicating an absence of correlation between the two bands. We try to explain the result as follows.

First, there are daily data for the X-ray band, yet the optical observations have not been performed regularly: 77 daily average points in 1187 days in total. The time resolution of our optical data is not compatible with that of *Swift*/BAT, which may possibly result in the loss of important fluctuations in the optical light curve, especially at the end of our monitoring program. It is probably difficult to find a strong correlation between two samples with very different sampling rates. Second, as shown

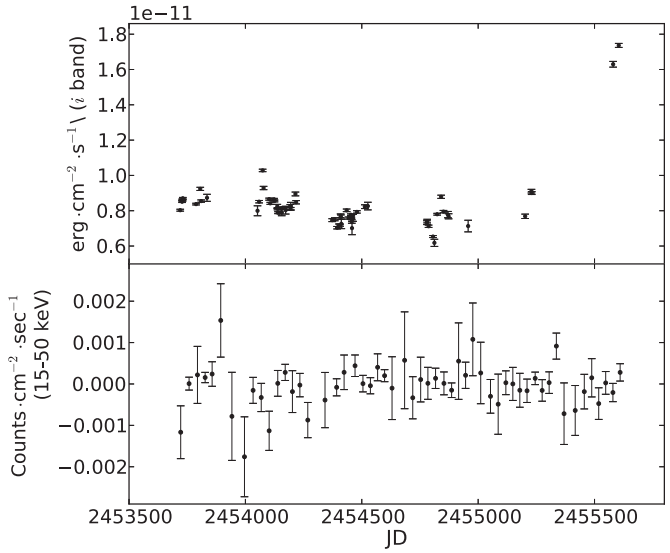

Figure 4. Light curve in the *i* band and X-ray band are shown here. Monthly average X-ray data were presented instead of the daily averages in order to provide a clearer view of the general variation in the graph.

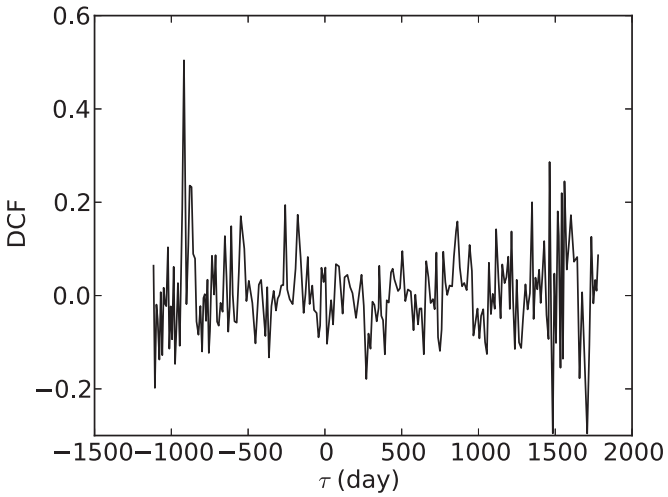

Figure 5. DCF of the z-transformed discrete correlation function.

in Figure 4, no significant flare or outburst can be found in both optical and X-ray bands. (There may be a strong flare at the end of the optical data, but the measurements are too few. The X-ray data obviously have no corresponding flare). As a result, it might be hard to find any correlation.

Third, provided that the no-correlation result is not caused by the limited data sampling in the optical band or the lack of significant variability events in both bands, it could be the reflection of a complex radiation mechanism. We notice that the hard-X-ray band from 3.63×10^{18} Hz to 1.21×10^{19} Hz lies in the transition area of the two peaks in the SED of 1ES 0806+52.4 (Cogan & VERITAS Collaboration 2008). Emission in this regime may be a combination of the synchrotron and inverse Compton mechanisms. Variations of the synchrotron and inverse Compton processes may have different amplitudes and cadences, hence a combination of them may show complicated variability and can hardly be found correlated with the optical variation. A similar explanation was raised to describe why the correlation between X-ray and other bands cannot be found in blazar S5 0716+714 (Rani et al. 2013).

Besides, there are also some other blazars showing no correlation between X-ray and other bands, which might be caused by the different locations of emission regions in different bands. For instance, 3C 279 was observed by Abdo et al. (2010), and its X-ray emission has not been found accompanied quasi-simultaneously by the optical/GeV flares. One argument is that X-ray photons are produced further down to the jet compared to optical–GeV photons. The case in which variations in the X-ray band are not correlated with those of the optical/gamma-ray (the so-called orphan gamma-ray flare) band was also found in other blazars such as Mrk 501 (Neronov et al. 2012), 1ES 1959+650 (Daniel et al. 2005), etc. The TeV flare in Mrk 501 may be produced by an electromagnetic cascade initiated by very-high-energy gamma-rays in the intergalactic medium (Neronov et al. 2012), and a hadronic synchrotron mirror model was employed to explain the orphan TeV flare of 1ES 1959+650 (Daniel et al. 2005). These results, together with ours, can be used to investigate the details of blazar variability, i.e., the radiation mechanism, the location of the emission region, etc.

6. CONCLUSIONS

Our monitoring work, which targeted the BL Lac object 1ES 0806+52.4, was conducted in five intermediate optical wavebands from 2005 December to 2011 February using the 60/90 cm Schmidt telescope located at the Xinglong Station of the NAOC. It was the first systematic multicolor optical monitoring of 1ES 0806+52.4 over a long timescale, and could thereby be effectively used to further study both the long- and short-term flux and spectral variability of this object.

The analysis of the data reveals that its overall brightness declined from 2005 December to 2008 December, and that it turned brighter during 2009–2011. Overlapping the long-term trend are some short-term small-amplitude oscillations. Unfortunately, our data samples are not abundant considering the long period of time that we covered, and there are several interruptions in our observation. No obvious intranight variability was found during the monitoring period, and the historical observation from 2002–2004 revealed the same feature. We did not find the double-peaked structure that the former observation suggested. Color behavior over long timescale was studied, and strong BWB phenomenon was revealed. This is consistent with the color behavior of most blazars. No obvious correlation was found between our optical variations and hard-X-ray variability collected from the *Swift*/BAT archive. This result can be attributed to the different time resolution of the optical and X-ray bands or the lack of a significant variability event in the observation session; moreover, it may suggest the hard-X-ray emission is a combination of both synchrotron radiation and inverse Compton scattering.

We gathered 1399 data points in total for 1ES 0806+52.4, which is the largest optical multicolor database for the variability of the object to date. Our data can also be correlated with the data aside from the hard-X-ray wavelength, e.g., radio, Gamma-ray, etc. for a more comprehensive investigation of the broadband behavior of 1ES 0806+52.4.

We thank the anonymous referee for insightful comments and constructive suggestions, and we also thank Yang Chen for his advice and help. Our work has been supported by the National Basic Research Program of China 973 Program 2013CB834900; Chinese National Natural Science Foundation grants 11273006, 11173016, and 11073023; and the fundamental research funds for the central universities and Beijing Normal University.

REFERENCES

Abdo, A. A., Ackermann, M., Ajello, M., et al. 2010, Natur, 463, 919
Aharonian, F., Akhperjanian, A., Beilicke, M., et al. 2004, A&A, 421, 529
Alexander, T. 1997, in Astronomical Time Series, ed. D. Maoz, A. Sternberg, & E. M. Leibowitz (Astrophysics and Space Science Library, Vol. 218; Dordrecht: Kluwer), 163
Bade, N., Beckmann, V., Douglas, N. G., et al. 1998, A&A, 334, 459
Becker, R. H., White, R. L., & Edwards, A. L. 1991, ApJS, 75, 1
Bonning, E., Urry, C. M., Bailyn, C., et al. 2012, ApJ, 756, 13
Cogan, P., & VERITAS Collaboration. 2008, in AIP Conf. Ser. 1085, Proc. of the 4th International Meeting on High Energy Gamma-ray Astronomy, ed. F. A. Aharonian, W. Hofmann, & F. Rieger (Melville, NY: AIP), 403
Dai, Y., Wu, J., Zhu, Z.-H., Zhou, X., & Ma, J. 2011, AJ, 141, 65
Dai, Y., Wu, J., Zhu, Z.-H., et al. 2013, ApJS, 204, 22
Daniel, M. K., Badran, H. M., Bond, I. H., et al. 2005, ApJ, 621, 181
de Diego, J. A. 2010, AJ, 139, 1269
de la Calle Pérez, I., Bond, I. H., Boyle, P. J., et al. 2003, ApJ, 599, 909
Edelson, R. A., & Krolik, J. H. 1988, ApJ, 333, 646
Elvis, M., Plummer, D., Schachter, J., & Fabbiano, G. 1992, ApJS, 80, 257
Fan, X., Burstein, D., Chen, J.-S., et al. 1996, AJ, 112, 628
Fiorucci, M., Tosti, G., & Rizzi, N. 1998, PASP, 110, 105
Gaskell, C. M., & Peterson, B. M. 1987, ApJS, 65, 1
Gaur, H., Gupta, A. C., Wiita, P. J., et al. 2014, ApJL, 781, L4
Gu, M. F., & Ai, Y. L. 2011, A&A, 534, A59
Gu, M. F., Lee, C.-U., Pak, S., Yim, H. S., & Fletcher, A. B. 2006, A&A, 450, 39
Hagen-Thorn, V. A., Larionov, V. M., Jorstad, S. G., et al. 2008, ApJ, 672, 40
Horan, D., Badran, H. M., Bond, I. H., et al. 2004, ApJ, 603, 51
Howell, S. B., Warnock, A., III, & Mitchell, K. J. 1988, AJ, 95, 247
Hu, S. M., Zhao, G., Guo, H. Y., Zhang, X., & Zheng, Y. G. 2006, MNRAS, 371, 1243
Kapanadze, B. Z. 2009, MNRAS, 398, 832
Krawczynski, H., Coppi, P. S., & Aharonian, F. 2002, MNRAS, 336, 721
Krimm, H. A., Holland, S. T., Corbet, R. H. D., et al. 2013, ApJS, 209, 14
Kurtanidze, O. M., Nikolashvili, M. G., Richter, G. M., & Sigua, L. A. 2002, in X-ray Spectroscopy of AGN with *Chandra* and *XMM-Newton*, ed. T. Boller, S. Komossa, S. Kahn, H. Kunieda, & L. Gallo, 301
Levinson, A. 2006, IJMPA, 21, 6015
Mücke, A., & Protheroe, R. J. 2001, APh, 15, 121
Mücke, A., Protheroe, R. J., Engel, R., Rachen, J. P., & Stanev, T. 2003, APh, 18, 593
Neronov, A., Semikoz, D., & Taylor, A. M. 2012, A&A, 541, A31
Oke, J. B., & Gunn, J. E. 1983, ApJ, 266, 713
Rani, B., Gupta, A. C., Strigachev, A., et al. 2010, MNRAS, 404, 1992
Rani, B., Krichbaum, T. P., Fuhrmann, L., et al. 2013, A&A, 552, A11
Sandrinelli, A., Covino, S., & Treves, A. 2014, A&A, 562, A79
Sasada, M., Uemura, M., Arai, A., et al. 2008, PASJ, 60, L37
Schachter, J. F., Stocke, J. T., Perlman, E., et al. 1993, ApJ, 412, 541
Stetson, P. B. 1987, PASP, 99, 191
Takahashi, T. 2001, in AIP Conf. Ser. 558, High Energy Gamma-ray Astronomy: International Symp., ed. F. A. Aharonian & H. J. Völk (Melville, NY: AIP), 346
Vagnetti, F., Trevese, D., & Nesci, R. 2003, ApJ, 590, 123
Weekes, T. C., Badran, H., Biller, S. D., et al. 2002, APh, 17, 221
Wu, J., Peng, B., Zhou, X., et al. 2005, AJ, 129, 1818
Yan, H., Burstein, D., Fan, X., et al. 2000, PASP, 112, 691
Zhai, M., & Wei, J. Y. 2012, A&A, 538, A125
Zheng, Z., Shang, Z., Su, H., et al. 1999, AJ, 117, 2757
Zhou, X., Jiang, Z., Ma, J., et al. 2003, A&A, 397, 361
Zhou, X., Jiang, Z.-J., Xue, S.-J., et al. 2001, ChJAA, 1, 372